



Hippocampal degeneration is associated with temporal and limbic gray matter/white matter tissue contrast in Alzheimer's disease

D.H. Salat^{a,b,c,*}, J.J. Chen^{a,b}, A.J. van der Kouwe^{a,b}, D.N. Greve^{a,b}, B. Fischl^{a,b,d}, H.D. Rosas^{a,e}

^a Athinoula A. Martinos Center for Biomedical Imaging, Charlestown, MA, USA

^b Department of Radiology, Massachusetts General Hospital, Boston, MA, USA

^c Neuroimaging Research for Veterans Center, VA Boston Healthcare System, Boston, MA, USA

^d Computer Science and Artificial Intelligence Laboratory, Massachusetts Institute of Technology, Cambridge, MA, USA

^e Department of Neurology, Massachusetts General Hospital, Boston, MA, USA

ARTICLE INFO

Article history:

Received 17 May 2010

Revised 17 September 2010

Accepted 11 October 2010

Available online 18 October 2010

Keywords:

Alzheimer's disease

Cerebral cortex

Cortical thickness

Gray matter

Cortical surface

Tissue contrast

Pathology

Aging

Medial temporal

Entorhinal

Hippocampus

ABSTRACT

Recent studies have demonstrated alterations in cortical gray to white matter tissue contrast with nondemented aging and in individuals with Alzheimer's disease (AD). However, little information exists about the clinical relevance of such changes. It is possible that changes in MRI tissue contrast occur via independent mechanisms from those traditionally used in the assessment of AD associated degeneration such as hippocampal degeneration measured by more traditional volumetric magnetic resonance imaging (MRI). We created cortical surface models of 95 cognitively healthy individuals and 98 individuals with AD to characterize changes in regional gray and white matter T1-weighted signal intensities in dementia and to evaluate how such measures related to classically described hippocampal and cortical atrophy. We found a reduction in gray matter to white matter tissue contrast throughout portions of medial and lateral temporal cortical regions as well as in anatomically associated regions including the posterior cingulate, precuneus, and medial frontal cortex. Decreases in tissue contrast were associated with hippocampal volume, however, the regional patterns of these associations differed for demented and nondemented individuals. In nondemented controls, lower hippocampal volume was associated with decreased gray/white matter tissue contrast globally across the cortical mantle. In contrast, in individuals with AD, selective associations were found between hippocampal volume and tissue contrast in temporal and limbic tissue. These results demonstrate that there are strong regional changes in neural tissue properties in AD which follow a spatial pattern including regions known to be affected from pathology studies. Such changes are associated with traditional imaging metrics of degeneration and may provide a unique biomarker of the tissue loss that occurs as a result of AD.

Published by Elsevier Inc.

Introduction

Prior studies have demonstrated the effect of AD on several neuroimaging parameters of tissue integrity, including alterations in cortical morphometry and volume (Fotenos et al., 2005; Jernigan et al., 1991b; Thompson et al., 1998) and cortical thickness (Dickerson et al., 2009; Lerch et al., 2008; Lerch et al., 2005), as well as regional changes in tissue properties such as tissue microstructure measured by diffusion tensor imaging (DTI) (Bozzali et al., 2002; Bozzali et al., 2001; Head et al., 2004; Rose et al., 2000; Salat et al. 2010). Less studied in AD are changes in tissue signal properties, such as T1 relaxation times and signal intensity which have been examined more extensively in nondemented aging (Cho et al., 1997; Davatzikos and

Resnick, 2002; Ogg and Steen, 1998; Raz et al., 1990; Salat et al., 2009; Steen et al., 1995; Westlye et al., 2009) and to some extent in AD (Westlye et al., 2009). While MRI tissue signal changes in individuals with AD have been demonstrated (Westlye et al., 2009), the association between contrast changes and more traditional metrics of degeneration in AD has thus far been completely unexplored.

In order to characterize the unique changes in tissue characteristics in AD, we created cortical surface models in a large sample of nondemented individuals and individuals with a clinical diagnosis of AD. Surface models were utilized to map gray and white matter signal intensities from high-resolution 3D T1-weighted MPRAGE images to examine the regional patterns of AD-specific associated signal alterations. This is a unique measure that can only be calculated with the creation of explicit models of the gray matter/white matter and gray matter/cerebrospinal fluid borders for a regional assessment of true tissue contrast. We additionally examined the association between this novel metric of tissue changes and traditional metrics of AD pathology including hippocampal volume and cortical thickness, and Clinical

* Corresponding author. MGH/MIT/HMS Athinoula A. Martinos Center for Biomedical Imaging, MGH Dept. Radiology, Building 149, 13th St. Mail Code 149 (2301), Charlestown, MA 02129-2060, USA. Fax: +1 617 726 7422.

E-mail address: salat@nmr.mgh.harvard.edu (D.H. Salat).

Dementia Rating (CDR) as a measure of dementia severity. We specifically focused on the gray to white matter signal intensity ratio (GWR) at each point along the cortical surface to determine whether contrast properties were altered in a regionally specific manner throughout the brain. The GWR showed a considerable increase (towards a value of 1) with increasing severity of AD, demonstrating an overall decrease in the contrast between tissue classes. These findings demonstrate that tissue signal properties are altered in AD in a regionally specific manner. Such changes may be an indirect marker of changes in the histological properties of the tissue that have a significant impact on neural and cognitive processes. These findings may therefore have important clinical applications in the monitoring of degenerative effects resultant from AD. Alterations in tissue contrast remained when controlling for changes in morphometric properties, suggesting that the novel GWR metric may provide a unique *in vivo* biomarker of degenerative changes in AD.

Materials and methods

Participants

Images were obtained for 193 participants (Table 1). All older nondemented adults and individuals with ADs were recruited and clinically evaluated through the Washington University Alzheimer's Disease Research Center (ADRC) as reported previously (Berg et al., 1998; Morris, 1993). These data are publically accessible as part of the Open Access Series of Imaging Studies (OASIS: <http://www.oasis-brains.org/>). Nondemented individuals were all clinically screened to ensure no signs of even mild cognitive impairment (all CDR 0). Fotenos et al. (2005) describe the recruitment characteristics of this sample in detail. Participants consented in accordance with guidelines of the Washington University Human Studies Committee.

MR acquisition and analysis

Signal properties were examined from high-resolution 3D MP-RAGE and cortical reconstruction procedures similar to descriptions in our prior work using cortical reconstruction (Dickerson et al., 2008; Han et al., 2006; Rosas et al., 2008; Salat et al., 2004; Salat et al., 2009) and intensity analysis (Salat et al., 2009). Two to five T1 weighted MP-RAGE scans per participant were acquired on a single scanner (Siemens 1.5 T Vision System, resolution $1 \times 1 \times 1.25$ mm, TR = 9.7 ms, TI = 20 ms, TE = 4.0 ms) motion corrected, and averaged to create high signal/contrast to noise volumes.

Cortical reconstruction was performed using the FreeSurfer image analysis suite, which is documented and freely available for download online (<http://surfer.nmr.mgh.harvard.edu/>). The technical details of these procedures are described in prior publications (Dale et al., 1999; Dale and Sereno, 1993; Fischl and Dale, 2000; Fischl et al., 2001; Fischl et al., 2002; Fischl et al., 2004a; Fischl et al., 1999a; Fischl et al., 1999b; Fischl et al., 2004b; Han et al., 2006; Jovicich et al., 2006; Segonne et al., 2004). Briefly, this processing includes removal of non-brain tissue using a hybrid watershed/surface deformation procedure (Segonne et al., 2004), automated Talairach transformation, segmentation of the subcortical white matter and deep gray matter volumetric structures (including hippocampus, amygdala, caudate, putamen, ventricles) (Fischl et al., 2002; Fischl et al., 2004a) intensity normalization (Sled et al., 1998), tessellation of the gray matter/white

matter boundary, automated topology correction (Fischl et al., 2001; Segonne et al., 2007), and surface deformation following intensity gradients to optimally place the gray/white and gray/CSF borders at the locations where the greatest shifts in intensity defines the transition to the other tissue class (Dale et al., 1999; Dale and Sereno, 1993; Fischl and Dale, 2000). Once the cortical models are complete, a number of deformable procedures are performed for further data processing and analysis including surface inflation (Fischl et al., 1999a), registration to a spherical atlas which utilizes individual cortical folding patterns to match cortical geometry across subjects (Fischl et al., 1999b), parcellation of the cerebral cortex into units based on gyral and sulcal structure (Desikan et al., 2006; Fischl et al., 2004b), and creation of a variety of surface based data including maps of curvature and sulcal depth. These procedures have been demonstrated to align histological properties such as cytoarchitectonic borders with greater accuracy than volumetric registration (Fischl et al., 2008). This method uses both intensity and continuity information from the entire three dimensional MR volume in segmentation and deformation procedures to produce representations of cortical thickness, calculated as the closest distance from the gray/white boundary to the gray/CSF boundary at each vertex on the tessellated surface (Fischl and Dale, 2000). The maps are created using spatial intensity gradients across tissue classes and are therefore not simply reliant on absolute signal intensity. The maps produced are not restricted to the voxel resolution of the original data and are thus capable of detecting submillimeter differences in thickness between groups. Procedures for the measurement of cortical thickness have been validated against histological analysis (Rosas et al., 2002) and manual measurements (Kuperberg et al., 2003; Salat et al., 2004). Freesurfer morphometric procedures have been demonstrated to show excellent test–retest reliability across scanner manufacturers and across field strengths and other imaging parameters (Han et al., 2006; Jovicich et al., 2009; Wonderlick et al., 2008). Images were corrected for intensity nonuniformity prior to sampling tissue intensities (Sled et al., 1998) to reduce the influence of inhomogeneity caused by B1 and coil profiles. In addition to this nonuniformity correction, examination of the GWR provided a highly localized (most voxels within ~2 mm) normalization of tissue values because the gray and white matter intensity from closely neighboring voxels would be expected to be similarly influenced by any imaging parameters due to the smoothness of the nuisance parameter maps (e.g. field B0/B1 inhomogeneities) which can be assumed to be smooth relative to the local normalization operation. Thus, presenting the gray matter values as a ratio to bordering white matter values provides a unit which is normalized for the local imaging environment.

Gray matter tissue intensities were measured at a depth of 35% through the thickness of the cortical ribbon, starting from the gray matter/white matter border and projecting towards the gray matter/cerebrospinal fluid border (Fig. 1). White matter signal intensities were sampled at 1 mm subjacent to the gray matter/white matter border. The 35% sampling procedure was utilized to be conservatively close to the gray/white border and the white matter sampling voxel (in order to minimize potential spurious effects that could arise in sampling from more remote locations and from sampling in regions of low cortical thickness). After calculation of the GWR, values were smoothed with a Gaussian kernel of FWHM 30 mm for analysis utilizing a surface based smoothing procedure that averages data across neighboring cortical locations. In contrast to 3D volumetric smoothing, the use of surface based smoothing limited the integration of information to regions limited by the area along the cortical mantle, preventing combining of data across sulcal space and cerebrospinal fluid.

Statistical analysis

The relationships among surface measures (GWR, and thickness) and AD were examined with a vertex by vertex general linear model

Table 1
Participant demographics.

Group	N	Age	MMSE
CDR = 0	95 (69F/26M)	76.21 ± 8.81 (61–94)	28.94 ± 1.25
CDR = 0.5	70 (39F/31M)	76.21 ± 7.19 (62–92)	25.64 ± 3.50
CDR = 1	28 (19F/9M)	77.75 ± 6.99 (65–96)	21.68 ± 3.75

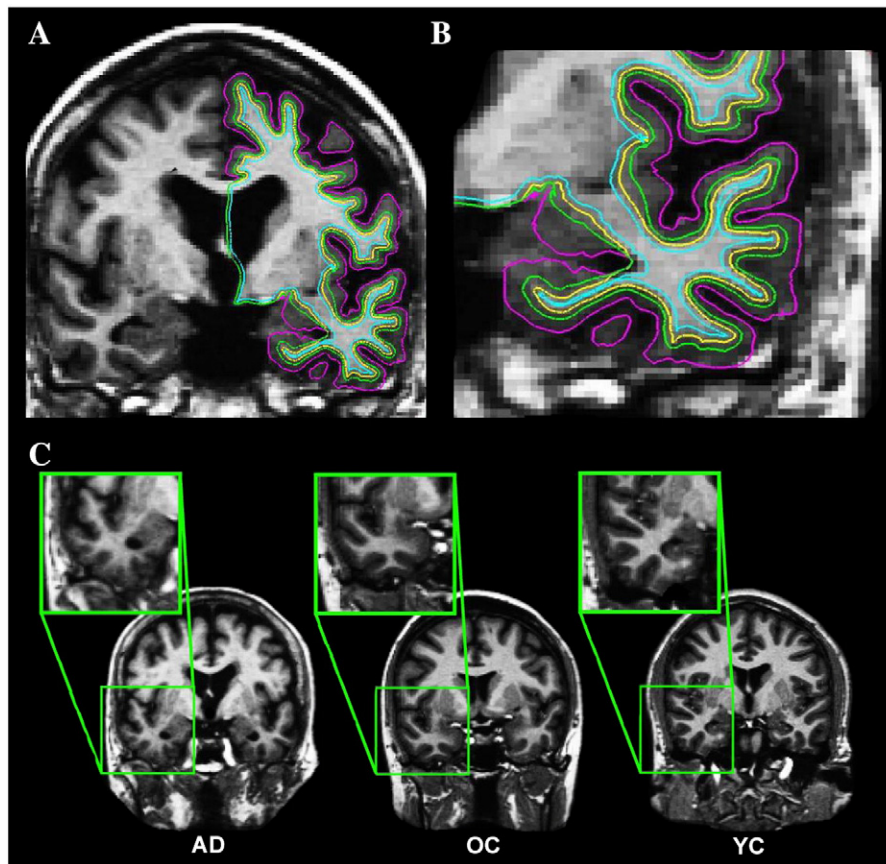


Fig. 1. Method for measuring tissue contrast. A–B. Gray matter tissue intensities (green surfaces; A, and in a magnified view in B, were measured at a depth of 35% through the thickness of the cortical ribbon, starting from the gray matter/white matter border (yellow surfaces) projecting towards the gray matter/cerebrospinal fluid border (purple surfaces), and 1 mm subjacent to the gray/white border for white matter (blue surfaces). The 35% sampling procedure was utilized to be conservatively close to the gray/white border and the white matter sampling voxel (in order to minimize potential spurious effects that could arise in sampling from more remote locations and from sampling in regions of low cortical thickness). C. Demonstration of the differential regional gray matter/white matter tissue contrast in an individual with Alzheimer's disease (AD), an older adult (OA), and a younger adult (YA).

(GLM). A separate GLM was evaluated for each vertex to assess regional variation in each measure. The significance of contrasts of the regression parameters was computed using *t*-tests. Additional models examined the association between hippocampal volume and tissue contrast.

Results

AD effects on regional signal intensities and contrast

Gray and white matter intensities were first normalized to the mean cortical intensity and compared between the demented and nondemented groups (Fig. 2). There was a regionally specific decrease in gray matter signal in cingulate and parahippocampal areas in AD compared to nondemented individuals. White matter signal was affected to a greater degree with decreased intensity throughout a large portion of the cortical mantle. The gray/white ratio (GWR) was significantly increased throughout portions of medial and lateral temporal cortex as well in regions including the cingulate and precuneus in individuals with AD compared to nondemented control participants.

Association between GWR and dementia severity (CDR)

Effects were strong when comparing the demented individuals to the nondemented control participants (Fig. 2, panels B–C). In contrast, only limited regions in medial temporal cortex differed in CDR 1 compared to CDR 0.5, suggesting that most tissue changes are present

early in the disease. However, small patches of inferior lateral and medial temporal regions demonstrated progressive changes in the GWR with increasing dementia severity (Fig. 2, panel D).

Association between hippocampal volume and GWR

There were strong associations between hippocampal volume and GWR in both healthy nondemented individuals and in patients with AD; however, the regional patterns of these associations differed. In nondemented individuals, more generalized regional increases in GWR were associated with reduced hippocampal volumes (Fig. 3B); in contrast, in demented individuals these associations were limited to medial and lateral temporal cortex (Fig. 3A). There was an interaction between demented and nondemented individuals when examining the association between hippocampal volume and GWR, with nondemented individuals showing a stronger association in most areas throughout the cortical mantle except for medial temporal and right lateral temporal areas (Fig. 4).

Association between GWR and cortical thickness

Fig. 5 demonstrates the effect of AD on GWR across all participants (CDR 1 and CDR 0.5 combined), and the effect of AD in the same individuals on cortical thickness. There was substantial regional overlap of the changes in these two metrics of tissue integrity with AD. Fig. 5C demonstrates the effect of AD on GWR while controlling for the cortical thickness at each vertex along the cortical mantle.

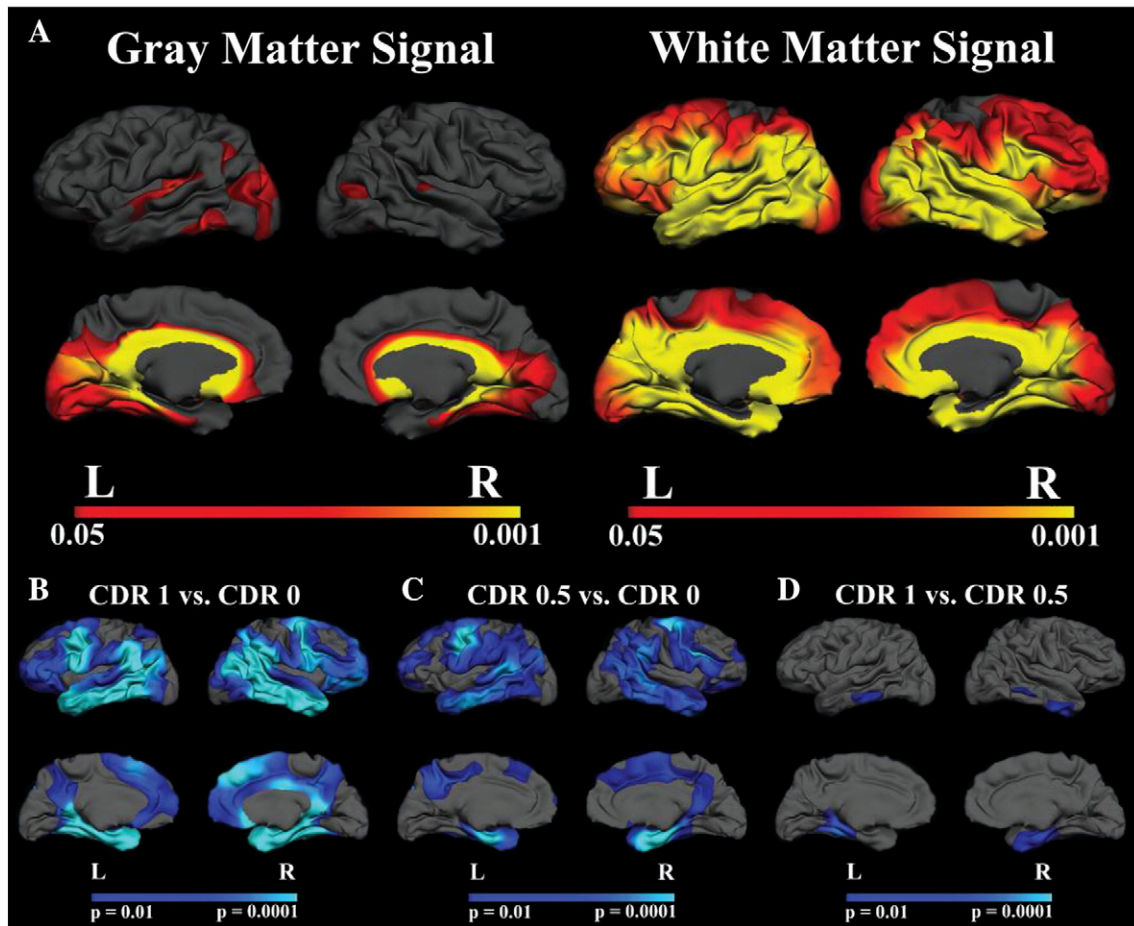


Fig. 2. A. Effect of AD on gray and white matter signal normalized to mean cortical gray matter signal intensity. AD showed limited regional effects in gray matter signal (left panel), however, white matter intensity was decreased in AD throughout a large portion of the cerebral mantle. B–D. Group comparisons of GWR in Demented and Nondemented Individuals. There was a significant effect on GWR in individuals with AD. CDR 1 and CDR 0.5 showed similar patterns of regionally distinct increases in GWR (contrast decreased) compared to nondemented controls (B–C). There were minimal effects on the GWR with increasing dementia severity. CDR 0.5 compared to CDR 1 showed significant changes in inferior lateral and medial temporal regions demonstrating modest progressive changes in the GWR with increasing dementia severity (D). Maps of the effect of AD on GWR were thresholded at $p < 0.01$.

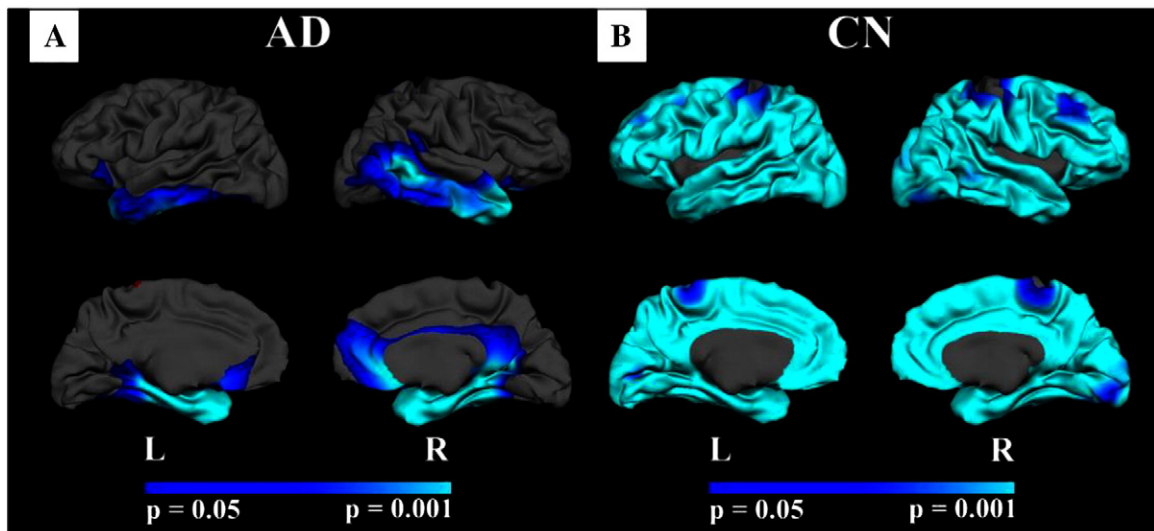


Fig. 3. Correlation between hippocampal volume and GWR in AD and nondemented control participants (CN). A. The association between hippocampal volume (corrected for ICV) and GWR in AD (CDR 1 and CDR 0.5 combined) B. The same association in control participants (CN; CDR 0).

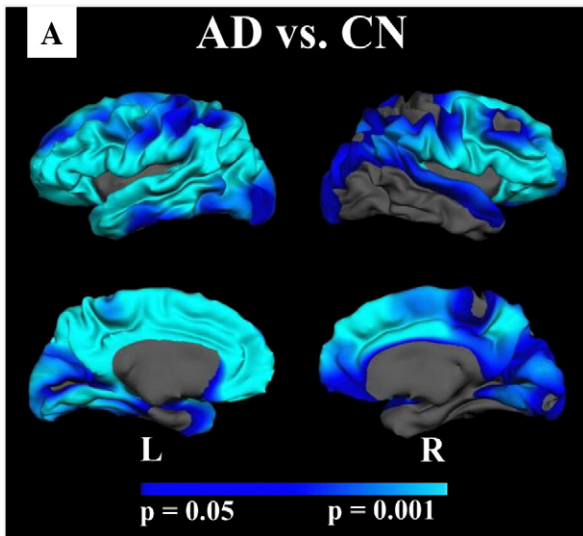


Fig. 4. Interaction between GWR and mean hippocampal volume in AD and CN participants. There were strong group by hippocampal volume interactions on GWR. These results demonstrate that whereas hippocampal volume is a predictor of GWR throughout a large portion of the cortex in nondemented individuals, this association is only similarly strong in medial and lateral temporal regions in AD.

These results demonstrate that the effects of AD on GWR are beyond the variance accounted for by cortical thickness alone.

Reliability of AD-associated changes in GWR

We performed a split sample analysis to examine the reliability of the AD associated effects in GWR. For this analysis, we sorted the demented group and the nondemented group individually by sex and then by age and assigned the odd numbered participants to group 1 and the even numbered participants to group 2 to create two equal age and sex matched samples. Differences in the GWR between demented and nondemented individuals were reliable across the two samples (Fig. 6), and were in accord with the overall group maps presented in Figs. 2 and 5.

Gyral versus sulcal effects on GWR

It is possible that the effects measured here could be influenced by gyral location (e.g. crown of a gyrus versus the fundus of a sulcus) for biological as well as for technical reasons. We therefore performed a secondary analysis to determine whether the effects of AD on GWR were influenced by gyral location by extracting unsmoothed GWR

data from two ROIs; one ROI limited to the gyral portion of a region affected by AD, and the other ROI limited to the sulcal portion of the same region. The effects were similar across the two ROIs (Fig. 7). Thus, although these results do not completely exclude the potential influence of curvature on the GWR measurements, they do demonstrate that the effects are not strictly limited to gyral or sulcal regions.

Discussion

The current results demonstrate that there are regionally selective alterations in MR image properties that occur uniquely with AD that are distinct from the effects from nondemented healthy aging. Individuals with AD exhibited reduced gray matter to white matter tissue contrast in several regions throughout the cortical mantle with particularly strong effects in temporal and limbic areas. In contrast, associations with hippocampal volume were only found in limited regions of temporal and parietal cortex, and the effects were statistically beyond what could be explained by cortical thinning. These results thus importantly suggest that tissue contrast measures may provide a more sensitive metric, or reflect a distinct pathology from the traditional measures of volume and thickness. These changes were found in individuals who were in early stages of AD (CDR 0.5), and may provide an indirect and sensitive metric of early histological or pathological processes.

Although prior studies have demonstrated changes in brain morphometry due to AD with various MRI analysis procedures, few studies have examined the effects of AD on tissue signal properties. Westlye et al. (2009) recently demonstrate that tissue properties could be used to enhance the effects of cortical thickness measurements in the study of AD. In addition to this, the current data suggest that the tissue properties are an interesting parameter to examine on their own; and that this metric correlates to some extent with more classical measures of pathology such as hippocampal volume. Although the effects of AD on GWR remained when considering effects on cortical thickness, there was substantial regional overlap between these metrics. Thus, GWR effects could be a microstructural marker of pathologic mechanisms that occur prior to cortical atrophy, and changes may occur with a distinct temporal pattern in the disease process; however it is currently unknown whether changes in GWR and thickness are due to similar or different biological mechanisms. Similarly, the current data do not address the relative strengths of GWR compared to traditional measures such as cortical thickness with regard to prediction of dementia. However, given the unique properties of the GWR measure, it is likely to be useful for understanding neural decline as well as to serve as biomarkers of early disease processes.

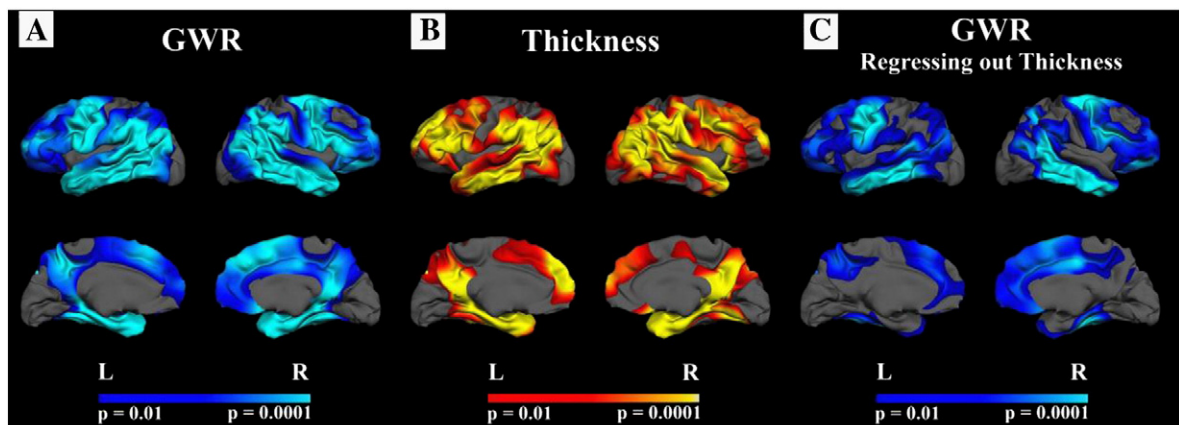


Fig. 5. Comparison of GWR and cortical thickness in AD. A–B. Changes in GWR with AD (CDR 1 and 0.5 combined) followed similar spatial patterns to those of cortical thinning. C. Group differences in GWR remained after controlling for thickness at each vertex along the cortical mantle suggesting some statistical independence of these measures.

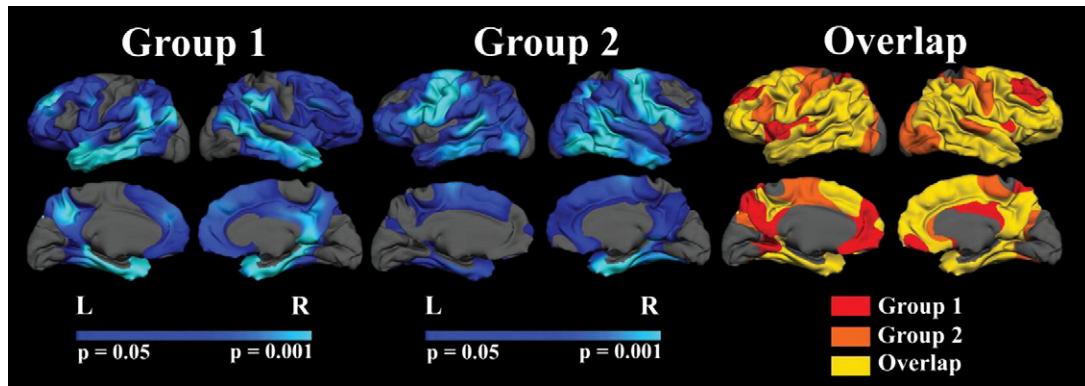


Fig. 6. Reliability of AD associated changes in GWR. A split sample analysis was performed by creating two independent gender and disease severity matched samples and performing the same analysis described in Fig. 2 on each of the split samples (Group 1 and Group 2). Overall, patterns of disease associated increases in GWR remained strong and the regions showing effects of AD were consistent across the two samples (Overlap; yellow).

Primary attention has been put towards gray matter degeneration in AD given the known early and primary pathology noted through histopathological analysis, particularly within the entorhinal cortex (Ball, 1978; Hyman et al., 1984). However, histological work (Hyman et al., 1984) as well as recent neuroimaging studies (Choo et al., 2008; Rose et al., 2006; Salat et al., 2008; Salat et al., 2010; Zhang et al., 2007) demonstrate that white matter within the parahippocampal gyrus is substantially affected in AD. It is possible that these white matter changes contribute to the change in tissue contrast, and that signal properties are influenced by tissue changes on a microstructural scale that presage the macrostructural effect of cortical atrophy or white matter tissue degradation. The tissue specific analyses suggested that changes in white matter signal intensity may contribute substantially to the changes in GWR observed. These results should be viewed with caution because the signal intensities examined were not from quantitative acquisitions and the specifics of the normalization procedures will influence the outcome. Overall, these findings suggest that intensity measures may be an important biomarker of aging and age-associated disease. It is therefore possible that intensity and contrast measures may be useful in diagnostic and other clinical procedures. We note that the effects of AD on GWR were both

spatially and statistically greatly reduced compared to the effects of age on GWR described in prior work (Salat et al., 2009). It is therefore possible that further development of the procedures for data acquisition and analysis will be necessary to fully exploit this potential biomarker of disease associated processes.

These data contribute to prior imaging studies describing a reduction in gray/white matter tissue contrast with aging (Davatzikos and Resnick, 2002; Jernigan et al., 1991a; Magnaldi et al., 1993; Raz et al., 1990; Salat et al., 2009; Westlye et al., 2009). There is a strong dependence of T1 relaxation times on regional iron concentration in the brain (Ogg and Steen, 1998), and subtle changes of this sort could contribute to the current results. It was somewhat surprising that hippocampal volume was strongly related to GWR generally throughout the brain in the nondemented older adults, and that the effect was more selective in the AD group. It is possible that hippocampal volume is a general marker of brain health in this population. When an aggressive process such as AD is present, the more generalized associations break down, and the hippocampus is instead tied more selectively to linked degenerative changes in temporal and limbic cortex. The effects measured were in regions where pathology has been reported in both gray and white matter. The spatial colocalization of these effects demonstrates that the effect measured is of pathologic significance associated with the primary disease process and not a more generic or global effect on tissue.

It is important to consider any potential technical contributions of changes in one measure, such as signal properties, to changes in another measure such as cortical thickness. It is possible that changes in cortical thickness influence contrast measures, or alternatively, changes in contrast influence cortical thickness measures. The specifics of the sampling do affect the results (e.g. how far through the cortex the gray matter signal is sampled), however, the major findings of this study are constant across a range of methods. There is also potential for bias of these procedures in regions of thinner or thicker cortex, and it is likely that the thickness of the cortex affects the measures somewhat. We demonstrated that thickness had some influence on the data, but that effects remained in GWR when thickness was considered in the analyses. Also, we demonstrated that there are similar effects in neighboring gyral (thicker) and sulcal (thinner) regions in tissue showing an effect of AD on GWR suggesting that thickness may have some influence, but is not a major component of the effects reported. It is important to note that the current results are cross-sectional, and ongoing work will examine the longitudinal effects of AD on the GWR. Additionally, the current study utilized a 3D MPRAGE sequence to define tissue intensities. This is a limitation as this sequence is not quantitative and the signal intensities can be affected by technical aspects of the scanning procedures. Indeed the parameters of the MPRAGE sequence were selected to maximize the

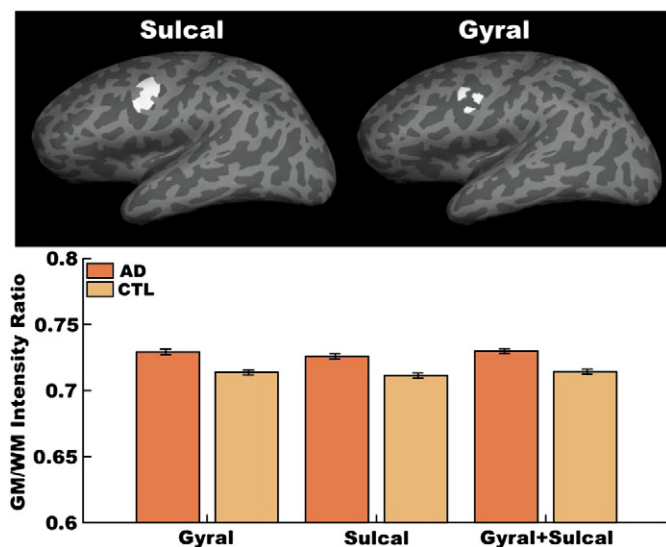


Fig. 7. Gyral versus sulcal effects on GWR. Unsmoothed GWR data were examined from two ROIs; one ROI limited to the sulcal portion of a region affected by AD (top left surface label, dark gray areas), and the other ROI limited to the gyral portion of the same region (top right surface label, light gray areas). The effects were similar across the two ROIs, and the results in each sub-ROI were similar to the full region.

sensitivity to differences between gray matter, white matter and CSF intensity per unit of acquisition time. Future work will examine changes in the GWR utilizing more optimized acquisition parameters for this type of analysis.

In summary, these results demonstrate changes in neural tissue signal properties with AD. These changes are regionally selective to areas known to show AD pathology, and were related to, yet statistically exceeding those of changes in morphometry. Thus, the GWR may be an important biomarker of pathologic changes with aging and disease and may reflect important histopathologic properties that will be of interest to examine in a range of studies to understand degenerative mechanisms and inform therapeutic intervention in AD.

Acknowledgments

This work was supported by the National Institutes of Health [K01AG024898, R01NR010827, P41RR14075, BIRN002, U24RR021382, R01EB001550, R01EB006758, R01NS052585, U54EB005149]; a postdoctoral fellowship from the Canadian Institutes of Health Research; the Athinoula A. Martinos Center for Biomedical Imaging, the Mental Illness and Neuroscience Discovery (MIND) Institute, and The Autism & Dyslexia Project funded by the Ellison Medical Foundation. We are grateful to Dr. Randy Buckner for his comments on this work, and for his support in the use of the OASIS dataset: Grants P50 AG05681, P01 AG03991, R01 AG021910, P50 MH071616, U24 RR021382, R01 MH56584.

References

- Ball, M.J., 1978. Topographic distribution of neurofibrillary tangles and granulovacuolar degeneration in hippocampal cortex of aging and demented patients. A quantitative study. *Acta Neuropathol* 42, 73–80.
- Berg, L., McKeel Jr., D.W., Miller, J.P., Storandt, M., Rubin, E.H., Morris, J.C., Baty, J., Coats, M., Norton, J., Goate, A.M., Price, J.L., Gearing, M., Mirra, S.S., Saunders, A.M., 1998. Clinicopathologic studies in cognitively healthy aging and Alzheimer's disease: relation of histologic markers to dementia severity, age, sex, and apolipoprotein E genotype. *Arch Neurol* 55, 326–335.
- Bozzali, M., Franceschi, M., Falini, A., Pontesilli, S., Cercignani, M., Magnani, G., Scotti, G., Comi, G., Filippi, M., 2001. Quantification of tissue damage in AD using diffusion tensor and magnetization transfer MRI. *Neurology* 57, 1135–1137.
- Bozzali, M., Falini, A., Franceschi, M., Cercignani, M., Zuffi, M., Scotti, G., Comi, G., Filippi, M., 2002. White matter damage in Alzheimer's disease assessed in vivo using diffusion tensor magnetic resonance imaging. *J Neurol Neurosurg Psychiatry* 72, 742–746.
- Cho, S., Jones, D., Reddick, W.E., Ogg, R.J., Steen, R.G., 1997. Establishing norms for age-related changes in proton T1 of human brain tissue in vivo. *Magn Reson Imaging* 15, 1133–1143.
- Choo, I.H., Lee, D.Y., Oh, J.S., Lee, J.S., Lee, D.S., Song, I.C., Youn, J.C., Kim, S.G., Kim, K.W., Jhoo, J.H., Woo, J.L., 2008. Posterior cingulate cortex atrophy and regional cingulum disruption in mild cognitive impairment and Alzheimer's disease. *Neurobiol Aging*.
- Dale, A.M., Sereno, M.I., 1993. Improved localization of cortical activity by combining EEG and MEG with MRI cortical surface reconstruction: a linear approach. *J Cogn Neurosci* 5, 162–176.
- Dale, A.M., Fischl, B., Sereno, M.I., 1999. Cortical surface-based analysis: I. Segmentation and surface reconstruction. *Neuroimage* 9, 179–194.
- Davatzikos, C., Resnick, S.M., 2002. Degenerative age changes in white matter connectivity visualized in vivo using magnetic resonance imaging. *Cereb Cortex* 12, 767–771.
- Desikan, R.S., Segonne, F., Fischl, B., Quinn, B.T., Dickerson, B.C., Blacker, D., Buckner, R.L., Dale, A.M., Maguire, R.P., Hyman, B.T., Albert, M.S., Killiany, R.J., 2006. An automated labeling system for subdividing the human cerebral cortex on MRI scans into gyral based regions of interest. *Neuroimage* 31, 968–980.
- Dickerson, B.C., Fenstermacher, E., Salat, D.H., Wolk, D.A., Maguire, R.P., Desikan, R., Pacheco, J., Quinn, B.T., Van der Kouwe, A., Greve, D.N., Blacker, D., Albert, M.S., Killiany, R.J., Fischl, B., 2008. Detection of cortical thickness correlates of cognitive performance: reliability across MRI scan sessions, scanners, and field strengths. *Neuroimage* 39, 10–18.
- Dickerson, B.C., Bakkour, A., Salat, D.H., Feczko, E., Pacheco, J., Greve, D.N., Grodzstein, F., Wright, C.I., Blacker, D., Rosas, H.D., Sperling, R.A., Atri, A., Growdon, J.H., Hyman, B.T., Morris, J.C., Fischl, B., Buckner, R.L., 2009. The cortical signature of Alzheimer's disease: regionally specific cortical thinning relates to symptom severity in very mild to mild AD dementia and is detectable in asymptomatic amyloid-positive individuals. *Cereb Cortex* 19, 497–510.
- Fischl, B., Dale, A.M., 2000. Measuring the thickness of the human cerebral cortex from magnetic resonance images. *Proc Natl Acad Sci USA* 97, 11050–11055.
- Fischl, B., Sereno, M.I., Dale, A.M., 1999a. Cortical surface-based analysis: II. Inflation, flattening, and a surface-based coordinate system. *Neuroimage* 9, 195–207.
- Fischl, B., Sereno, M.I., Tootell, R.B., Dale, A.M., 1999b. High-resolution intersubject averaging and a coordinate system for the cortical surface. *Hum Brain Mapp* 8, 272–284.
- Fischl, B., Liu, A., Dale, A.M., 2001. Automated manifold surgery: constructing geometrically accurate and topologically correct models of the human cerebral cortex. *IEEE Trans Med Imaging* 20, 70–80.
- Fischl, B., Salat, D.H., Busa, E., Albert, M., Dieterich, M., Haselgrove, C., van der Kouwe, A., Killiany, R., Kennedy, D., Klaveness, S., Montillo, A., Makris, N., Rosen, B., Dale, A.M., 2002. Whole brain segmentation: automated labeling of neuroanatomical structures in the human brain. *Neuron* 33, 341–355.
- Fischl, B., Salat, D.H., van der Kouwe, A.J., Makris, N., Segonne, F., Quinn, B.T., Dale, A.M., 2004a. Sequence-independent segmentation of magnetic resonance images. *Neuroimage* 23 (Suppl 1), S69–S84.
- Fischl, B., van der Kouwe, A., Destrieux, C., Halgren, E., Segonne, F., Salat, D.H., Busa, E., Seidman, L.J., Goldstein, J., Kennedy, D., Caviness, V., Makris, N., Rosen, B., Dale, A.M., 2004b. Automatically parcellating the human cerebral cortex. *Cereb Cortex* 14, 11–22.
- Fischl, B., Rajendran, N., Busa, E., Augustinack, J., Hinds, O., Yeo, B.T., Mohlberg, H., Amunts, K., Zilles, K., 2008. Cortical folding patterns and predicting cytoarchitecture. *Cereb Cortex* 18, 1973–1980.
- Fotinos, A.F., Snyder, A.Z., Girton, L.E., Morris, J.C., Buckner, R.L., 2005. Normative estimates of cross-sectional and longitudinal brain volume decline in aging and AD. *Neurology* 64, 1032–1039.
- Han, X., Jovicich, J., Salat, D., van der Kouwe, A., Quinn, B., Czanner, S., Busa, E., Pacheco, J., Albert, M., Killiany, R., Maguire, P., Rosas, D., Makris, N., Dale, A., Dickerson, B., Fischl, B., 2006. Reliability of MRI-derived measurements of human cerebral cortical thickness: the effects of field strength, scanner upgrade and manufacturer. *Neuroimage* 32, 180–194.
- Head, D., Buckner, R.L., Shimony, J.S., Williams, L.E., Akbudak, E., Conturo, T.E., McAvoy, M., Morris, J.C., Snyder, A.Z., 2004. Differential vulnerability of anterior white matter in nondemented aging with minimal acceleration in dementia of the Alzheimer type: evidence from diffusion tensor imaging. *Cereb Cortex* 14, 410–423.
- Hyman, B.T., Van Hoesen, G.W., Damasio, A.R., Barnes, C.L., 1984. Alzheimer's disease: cell-specific pathology isolates the hippocampal formation. *Science* 225, 1168–1170.
- Jernigan, T.L., Archibald, S.L., Berhow, M.T., Sowell, E.R., Foster, D.S., Hesselink, J.R., 1991a. Cerebral structure on MRI: Part I. Localization of age-related changes. *Biol Psychiatry* 29, 55–67.
- Jernigan, T.L., Salmon, D.P., Butters, N., Hesselink, J.R., 1991b. Cerebral structure on MRI: Part II. Specific changes in Alzheimer's and Huntington's diseases. *Biol Psychiatry* 29, 68–81.
- Jovicich, J., Czanner, S., Greve, D., Haley, E., van der Kouwe, A., Gollub, R., Kennedy, D., Schmitt, F., Brown, G., Macfall, J., Fischl, B., Dale, A., 2006. Reliability in multi-site structural MRI studies: effects of gradient non-linearity correction on phantom and human data. *Neuroimage* 30, 436–443.
- Jovicich, J., Czanner, S., Han, X., Salat, D., van der Kouwe, A., Quinn, B., Pacheco, J., Albert, M., Killiany, R., Blacker, D., Maguire, P., Rosas, D., Makris, N., Gollub, R., Dale, A., Dickerson, B.C., Fischl, B., 2009. MRI-derived measurements of human subcortical, ventricular and intracranial brain volumes: reliability effects of scan sessions, acquisition sequences, data analyses, scanner upgrade, scanner vendors and field strengths. *Neuroimage* 46, 177–192.
- Kuperberg, G.R., Broome, M.R., McGuire, P.K., David, A.S., Eddy, M., Ozawa, F., Goff, D., West, W.C., Williams, S.C., van der Kouwe, A.J., Salat, D.H., Dale, A.M., Fischl, B., 2003. Regionally localized thinning of the cerebral cortex in schizophrenia. *Arch Gen Psychiatry* 60, 878–888.
- Lerch, J.P., Pruessner, J.C., Zijdenbos, A., Hampel, H., Teipel, S.J., Evans, A.C., 2005. Focal decline of cortical thickness in Alzheimer's disease identified by computational neuroanatomy. *Cereb Cortex* 15, 995–1001.
- Lerch, J.P., Pruessner, J., Zijdenbos, A.P., Collins, D.L., Teipel, S.J., Hampel, H., Evans, A.C., 2008. Automated cortical thickness measurements from MRI can accurately separate Alzheimer's patients from normal elderly controls. *Neurobiol Aging* 29, 23–30.
- Magnaldi, S., Ukmar, M., Vasciaveo, A., Longo, R., Pozzi-Mucelli, R.S., 1993. Contrast between white and grey matter: MRI appearance with ageing. *Eur Radiol* 513–519.
- Morris, J.C., 1993. The Clinical Dementia Rating (CDR): current version and scoring rules. *Neurology* 43, 2412–2414.
- Ogg, R.J., Steen, R.G., 1998. Age-related changes in brain T1 are correlated with iron concentration. *Magn Reson Med* 40, 749–753.
- Raz, N., Millman, D., Sarpel, G., 1990. Cerebral correlates of cognitive aging: gray–white–matter differentiation in the medial temporal lobes, and fluid versus crystallized abilities. *Psychobiology* 18, 475–481.
- Rosas, H.D., Liu, A.K., Hersch, S., Glessner, M., Ferrante, R.J., Salat, D.H., van der Kouwe, A., Jenkins, B.G., Dale, A.M., Fischl, B., 2002. Regional and progressive thinning of the cortical ribbon in Huntington's disease. *Neurology* 58, 695–701.
- Rosas, H.D., Salat, D.H., Lee, S.Y., Zaleta, A.K., Pappu, V., Fischl, B., Greve, D., Hevelone, N., Hersch, S.M., 2008. Cerebral cortex and the clinical expression of Huntington's disease: complexity and heterogeneity. *Brain* 131, 1057–1068.
- Rose, S.E., Chen, F., Chalk, J.B., Zelaya, F.O., Strugnell, W.E., Benson, M., Semple, J., Doddrell, D.M., 2000. Loss of connectivity in Alzheimer's disease: an evaluation of white matter tract integrity with colour coded MR diffusion tensor imaging. *J Neurol Neurosurg Psychiatry* 69, 528–530.
- Rose, S.E., McMahon, K.L., Janke, A.L., O'Dowd, B., de Zubicaray, G., Strudwick, M.W., Chalk, J.B., 2006. Diffusion indices on magnetic resonance imaging and neuropsychological performance in amnesic mild cognitive impairment. *J Neurol Neurosurg Psychiatry* 77, 1122–1128.
- Salat, D.H., Buckner, R.L., Snyder, A.Z., Greve, D.N., Desikan, R.S., Busa, E., Morris, J.C., Dale, A.M., Fischl, B., 2004. Thinning of the cerebral cortex in aging. *Cereb Cortex* 14, 721–730.

- Salat, D.H., Greve, D.N., Pacheco, J.L., Quinn, B.T., Helmer, K.G., Buckner, R.L., Fischl, B., 2008. Regional white matter volume differences in nondemented aging and Alzheimer's disease. *Neuroimage*.
- Salat, D.H., Lee, S.Y., van der Kouwe, A.J., Greve, D.N., Fischl, B., Rosas, H.D., 2009. Age-associated alterations in cortical gray and white matter signal intensity and gray to white matter contrast. *Neuroimage* 48, 21–28.
- Salat, D.H., Tuch, D.S., van der Kouwe, A.J., Greve, D.N., Pappu, V., Lee, S.Y., Hevelone, N.D., Zaleta, A.K., Growdon, J.H., Corkin, S., Fischl, B., Rosas, H.D., 2010. White matter pathology isolates the hippocampal formation in Alzheimer's disease. *Neurobiol Aging* 31, 244–256.
- Segonne, F., Dale, A.M., Busa, E., Glessner, M., Salat, D., Hahn, H.K., Fischl, B., 2004. A hybrid approach to the skull stripping problem in MRI. *Neuroimage* 22, 1060–1075.
- Segonne, F., Pacheco, J., Fischl, B., 2007. Geometrically accurate topology-correction of cortical surfaces using nonseparating loops. *IEEE Trans Med Imaging* 26, 518–529.
- Sled, J.G., Zijdenbos, A.P., Evans, A.C., 1998. A nonparametric method for automatic correction of intensity nonuniformity in MRI data. *IEEE Trans Med Imaging* 17, 87–97.
- Steen, R.G., Gronemeyer, S.A., Taylor, J.S., 1995. Age-related changes in proton T1 values of normal human brain. *J Magn Reson Imaging* 5, 43–48.
- Thompson, P.M., Moussai, J., Zohoori, S., Goldkorn, A., Khan, A.A., Mega, M.S., Small, G.W., Cummings, J.L., Toga, A.W., 1998. Cortical variability and asymmetry in normal aging and Alzheimer's disease. *Cereb Cortex* 8, 492–509.
- Westlye, L.T., Walhovd, K.B., Dale, A.M., Espeseth, T., Reinvang, I., Raz, N., Agartz, I., Greve, D.N., Fischl, B., Fjell, A.M., 2009. Increased sensitivity to effects of normal aging and Alzheimer's disease on cortical thickness by adjustment for local variability in gray/white contrast: a multi-sample MRI study. *Neuroimage* 47, 1545–1557.
- Wonderlick, J.S., Ziegler, D.A., Hosseini-Varnamkhandi, P., Locascio, J.J., Bakkour, A., van der Kouwe, A., Triantafyllou, C., Corkin, S., Dickerson, B.C., 2008. Reliability of MRI-derived cortical and subcortical morphometric measures: effects of pulse sequence, voxel geometry, and parallel imaging. *Neuroimage*.
- Zhang, Y., Schuff, N., Jahng, G.H., Bayne, W., Mori, S., Schad, L., Mueller, S., Du, A.T., Kramer, J.H., Yaffe, K., Chui, H., Jagust, W.J., Miller, B.L., Weiner, M.W., 2007. Diffusion tensor imaging of cingulum fibers in mild cognitive impairment and Alzheimer disease. *Neurology* 68, 13–19.